JACC: CARDIOVASCULAR IMAGING VOL. 3, NO. 7, 2010

ISSN 1936-878X/$36.00
PUBLISHED BY ELSEVIER INC. DOI:10.1016/j.jcmg.2010.03.008

Relationship Between Transmural Extent of Necrosis and Quantitative Recovery of Regional Strains After Revascularization

Bernhard L. Gerber, MD, Julie Darchis, MD, Jean-Benoît le Polain de Waroux, MD, Gabin Legros, MD, Anne-Catherine Pouleur, MD, David Vancraeynest, MD, Agnès Pasquet, MD, Jean-Louis Vanoverschelde, MD

Brussels, Belgium

OBJECTIVES To better understand the quantitative relationship of recovery of regional and global dysfunction after revascularization in chronic infarcts with variable transmural extent of necrosis by delayed enhanced cardiac magnetic resonance.

BACKGROUND Studies relating transmurality of delayed enhanced magnetic resonance to functional recovery in dysfunctional myocardium using semiquantitative Likert scales have demonstrated the intermediate likelihood (50% probability) of recovery of dysfunction in subendocardial scars.

METHODS Forty-two patients with chronic left ventricular dysfunction due to coronary artery disease underwent tagged and delayed enhanced magnetic resonance before and 10 ± 7 months after revascularization (coronary artery bypass graft: 35, percutaneous transluminal coronary angioplasty: 7). Left ventricular ejection fraction and regional mid-myocardial Eulerian radial thickening strain (Err) and mid-myocardial, subendocardial, and subepicardial Eulerian circumferential shortening strain (Ecc) strains were quantified in 16 segments per patient before and after revascularization and related to pre-operatively measured transmurality of necrosis.

RESULTS At baseline, 256 of 672 segments were dysfunctional, having <2 SD (i.e., $>-10\%$) mid-myocardial Ecc. The magnitude of recovery of mid-myocardial Ecc ($r = -0.33$, $p < 0.01$) was inversely correlated with transmurality of necrosis before revascularization. Segments with $<25\%$ necrosis improved mid-myocardial Ecc and Err. No significant improvement of mid-myocardial Ecc or Err occurred when transmurality was $\geq 25\%$. However, subendocardial Ecc improved up to 75% transmural necrosis. Receiver-operator characteristic analysis determined optimal sensitivity (54%) and specificity (82%) for normalization of mid-myocardial Ecc (to $<-10\%$ Ecc) at a cutoff value of $\geq 18\%$ transmural necrosis. Improvement of left ventricular ejection fraction (from 35 ± 15% to 40 ± 7%, $p < 0.001$) was best predicted (67% sensitivity, 58% specificity) by the presence of <4.5 dysfunctional segments with $<75\%$ transmural necrosis.

CONCLUSIONS The quantitative relationship between necrosis transmurality and improvement of regional and global dysfunction after revascularization is complex. Although improvement of recovery of regional mid-myocardial dysfunction after revascularization was observed only for scarring not exceeding 25% transmurality, global dysfunction significantly improved even when more extensive subendocardial scarring was revascularized. (J Am Coll Cardiol Img 2010;3:720–30) © 2010 by the American College of Cardiology Foundation

From the Division of Cardiology, Cliniques Universitaires St. Luc, Brussels, Belgium. Grant support by the Fondation Nationale de la Recherche Scientifique of the Belgian Government (FRSM 3.4557.02). Contrast media for cardiac magnetic resonance was donated by Amersham-Nycomed (now GE Healthcare).

Manuscript received January 26, 2010; revised manuscript received March 29, 2010; accepted March 31, 2010.

Several studies have evaluated the value of delayed enhancement (DE) cardiac magnetic resonance (CMR) for assessment of myocardial viability in chronic ischemic dysfunction (1,2). They described an inverse relationship between the transmural extent of necrosis and likelihood of improvement of regional contractility after revascularization. Segments with high (75% to 100%) transmurality of necrosis were shown to be unable to recover function after revascularization, whereas segments with no or very little necrosis were found to likely improve function after revascularization. In segments with subendocardial scarring of 25% to 75% transmurality of DE, however, the likelihood of recovery of function was found to be intermediate, around 50%, and thus DE-CMR has a low accuracy in predicting functional recovery in such segments (3).

See page 731

However, a major limitation of earlier studies was that both the transmural extent of DE and the amount of functional recovery were assessed visually, using semiquantitative Likert scales. We hypothesized that the binary nature of assessment of necrosis and functional recovery might explain the uncertainty of predicting viability in such segments with subendocardial necrosis, and therefore we attempted to examine the relationship of the quantitatively transmural extent of DE using automated software to the magnitude of quantitatively measured regional myocardial strains obtained from tagged CMR images.

METHODS

Patients and study protocol. This prospective study enrolled consecutive patients with chronic regional contractile dysfunction in areas supplied by a severely stenotic or occluded coronary artery with clinical indication for revascularization by either percutaneous transluminal coronary angioplasty or coronary artery bypass graft (CABG). Patients who had an acute myocardial infarction within the past 30 days, hemodynamic instability, higher than grade II mitral or aortic insufficiency, significant aortic stenosis, chronic atrial fibrillation, or contraindications to CMR were not considered for inclusion.

Patients underwent tagged and DE-CMR before and >4 months after revascularization. Verification of completeness of revascularization was encouraged using either recatheterization or multidetector computed tomography (MDCT), if no contraindication (i.e., serum creatinine level >1.4 mg/dl) was present. Study enrollment is shown in Figure 1. Sixty-one patients underwent baseline CMR. Five patients died during follow-up, and 14 refused follow-up. The final study population consisted of 42 consecutive patients (Table 1). There were no significant differences in the patients who completed the protocol and those who were lost to follow-up. All participants gave informed consent for the study protocol, which had been approved by the institutional review board of our university.

Baseline coronary angiography. Coronary angiography was evaluated visually and semiquantitatively by a blinded reviewer using the standard 16-segment American Heart Association classification system (4). Luminal narrowing exceeding 50% of the mean reference luminal diameter was considered significant.

CMR protocol. CMR was performed as previously described (5). To compute regional strains, we acquired 6 to 8 contiguous short-axis images covering the entire left ventricle (LV) from base to apex with a prospectively triggered cine sequence with grid tagging. Subsequently, to assess LV function, we acquired retrospectively gated steady-state free-precession cine images. To evaluate myocardial viability, 2- or 3-dimensional DE images were acquired 15 min after administration of 0.20 mmol/kg^{-1} gadodiamide (Omniscan; GE Healthcare, Oslo, Norway) during mid-diastole. All images had the same orientation, slice thickness (8 mm), and spacing (2 mm) as the tagged short-axis images.

MDCT for verification of completeness of revascularization. To verify completeness of revascularization, 16- or 40-slice MDCT was performed as previously described (6). Patency of arterial and venous bypass grafts and stents was assessed visually by a blinded reviewer (B.G.).

Data analysis. REGISTRATION OF DATASETS. The sets of tagged and DE images acquired before revascularization were acquired using the same slice locations and thus did not need to be registered. Registration of CMR images before and after revascularization was performed using standard landmarks and facilitated by standardized acquisition covering the entire left ventricle. A standard American Heart Association 17-segment model omitting the apex (i.e., 16 segments per patient) was used to

ABBREVIATIONS AND ACRONYMS

AUC = area under the receiver-operator characteristic curve
CABG = coronary artery bypass graft
CI = confidence interval
CMR = cardiac magnetic resonance
DE = delayed enhancement
Ecc = Eulerian circumferential shortening strain
EF = ejection fraction
Err = Eulerian radial thickening strain
LV = left ventricle/ventricular
MDCT = multidetector CT

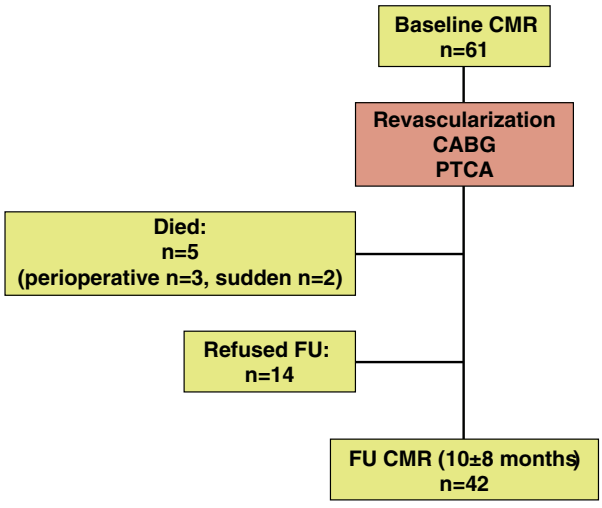

Figure 1. Illustration of the Study Cohort

Sixty-one patients underwent baseline cardiac magnetic resonance (CMR) before revascularization. Five patients died during follow-up (FU) and 14 refused FU. The final study population consisted of 42 consecutive patients who underwent a 10 ± 8 month FU study after revascularization. CABG = coronary artery bypass graft; PTCA = percutaneous transluminal coronary angioplasty.

interpret segmental strain and transmural DE on a regional basis. To obtain these 16 segments, 2 to 3 consecutive short-axis slices were assigned to the basal, mid-ventricular, and apical levels of the heart. The same number of slices was assigned to each level before and after revascularization. Using the inferoseptal insertion of the right ventricular wall as a landmark, each short-axis slice was subdivided into 4 (apex) or 6 (mid- and basal levels) radially spaced segments. Segments were assigned to coronary artery territories (7) according to standard criteria, taking into account the individual coronary anatomy of the patient (8). When the right coronary artery supplied at least 1 posterolateral branch, we assumed right coronary dominance and assigned the basal and inferoseptal and inferior segments to the right coronary artery. When the right coronary artery did not reach the crux cordis and when the inferior septal branches were supplied by the left coronary artery, we assumed left dominant circulation and assigned basal and inferoseptal and inferior segments to the left circumflex coronary artery.

REGIONAL STRAIN. Tagged images were analyzed using HARP (Diagnosoft, San Francisco, California). Within each of the 16 segments, mid-myocardial, subendocardial, and subepicardial Eulerian circumferential shortening strain (Ecc) and mid-myocardial Eulerian radial thickening strain (Err) were computed. Strains were expressed as the fractional change in myocardial length between end-diastole and end-systole. End-systole was defined as nadir of Ecc in normally contracting regions. The minimal (Ecc)/maximal (Err) strain in a range of 2 to 3 frames from end-systole was reported, excluding diastole to avoid measuring post-systolic strain. By convention, shortening strains had a negative sign and elongation strains positive. Normal values and interobserver and intraobserver reproducibility of mid-myocardial Ecc and Err were assessed in a previous study in 10 randomly selected patients (5). Both intraobserver and interobserver reproducibility had an intraclass correlation coefficient of 0.81. Mean values of mid-myocardial strain in normal healthy volunteers were Ecc -8 ± 4 (95% confidence interval [CI]: 10% to 26%) and Err 16 ± 5 (95% CI: 7% to 26.0%). Therefore, we defined regional contractile dysfunction as Ecc $<-10\%$ (i.e., lower 95% CIs in healthy volunteers) (5). Recovery of dysfunction was defined as return of Ecc or Err to lower 95% CIs of healthy volunteers (i.e., $<-10\%$ and $>7\%$ for Ecc and Err, respectively). Improvement of dysfunction was defined as improvement of Ecc or Err >95% CI of test-rest values of these measurements assessed in 5 healthy volunteers after 4 months. For Ecc, test-to-test variation was 0.5 ± 2.5 (95% CI: -4.3 to 5.5), intraclass correlation coefficient = 0.61. For Err, test-retest variation was 0.45 ± 4.1 (95% CI: -7.6 to 8.5), and reproducibility intraclass correlation coefficient = 0.73. Therefore, we defined significant improvement of function as improvement $<-5\%$ for Ecc or $>8\%$ for Err.

TRANSMURAL EXTENT OF INFARCTION. Assessment of the transmural extent of DE-CMR was performed using the freely available software Segment (9). After manually tracing endocardial and epicardial contours, the program semiautomatically detected and reported the mean transmural extent of DE in each of the 16 same segments that were used for computation of strain.

Global cardiac function. LV end-diastolic and end-systolic volumes and ejection fraction (EF) were obtained by manual tracing of endocardial contours on anonymized steady-state free-precession CMR images before and after revascularization. Measurements were performed in duplicate by 2 blinded observers, and the average measurement of both observers was reported.

Statistical analysis. All continuous values are reported as mean ± 1 SD. Only dysfunctional segments from territories with significant coronary

artery stenosis were considered for analysis. Segments belonging to nonrevascularized coronary territories and segments in which revascularization was incomplete due to documented graft or stent occlusion or restenosis by either recatheterization or MDCT were excluded from analysis. To correct for statistical independence of segments with different amounts of necrosis within patients, a mixed linear model was used to compare strains in remote and dysfunctional segments stratified according to quartiles of transmural infarction. The segment group (normo- or dysfunctional stratified by quartile of transmural extent of necrosis) was considered a fixed factor, whereas the patient was considered a random factor. Individual comparisons between sector groups were performed post hoc using Wilcoxon tests with a Bonferroni correction for multiple comparisons. Strain was also compared using Pearson regression analysis against transmural extent of necrosis in dysfunctional segments. Receiver-operator characteristic (ROC) curves were used to evaluate diagnostic accuracy of mean transmurality of necrosis to regional and global function. Optimal cutoff points were considered the greatest sum of sensitivity and specificity. All tests were 2 sided and a p value <0.05 was considered indicative of statistical significance.

RESULTS

Study population. The clinical characteristics of the patient population are shown in Table 1. Thirty-six (76%) patients had a history of myocardial infarction, occurring on average 54 ± 76 months (range 1 month to 20 years) before the study. Fourteen patients had infarcts <1 year ago. The majority of patients had multivessel disease and underwent revascularization with CABG. Two patients had left-main disease. At the time of the study, 37 vessels (11 left anterior descending, 9 left circumflex, and 17 right coronary arteries) were completely occluded, 47 had >75% diameter stenosis and 22 had 50% to 75% diameter stenosis.. Three patients had undergone previous revascularization (1 CABG and 2 percutaneous transluminal coronary angioplasty). Twenty patients had an EF <35%. Follow-up CMR was performed 10 ± 7 months (range 5 months to 4 years) after revascularization. No patient experienced a clinically significant event such as a new infarct, or revascularization between baseline and follow-up study.

Table 1. Baseline Characteristics of the Study Population

	Completed Follow-Up (n = 42)	Lost to Follow-Up (n = 19)	p Value
Age (yrs)	62 ± 9	67 ± 10	0.09 (NS)
Sex (M/F)	38/4	13/6	0.06 (NS)
Coronary risk factors			
Smoking	18 (42%)	7 (37%)	0.65 (NS)
Hypertension	26 (62%)	13 (68%)	0.62 (NS)
Diabetes mellitus	9 (21%)	8 (42%)	0.09 (NS)
Hypercholesterolemia	26 (62%)	9 (47%)	0.28 (NS)
Family history of CAD	13 (31%)	6 (31)	0.96 (NS)
No. of diseased vessels			
1	3 (7%)	2 (10%)	
2	14 (33%)	5 (26%)	
3	25 (60%)	12 (63%)	0.75 (NS)
Baseline CMR			
EDVI (ml/m^2)	116 ± 39	95 ± 35	0.65 (NS)
ESVI (ml/m^2)	79 ± 39	67 ± 34	0.76 (NS)
EF (%)	35 ± 13	33 ± 16	0.56 (NS)
Symptoms			
Chest pain	22 (53%)	5 (26%)	0.06 (NS)
Heart failure symptoms	18 (42%)	7 (37%)	0.65 (NS)
Previous MI	32 (76%)	12 (63%)	0.29 (NS)
Previous revascularization	3 (7%)	2 (10%)	0.64 (NS)
ECG			
Q waves	24 (57%)	13 (68%)	0.40 (NS)
LBBB	5 (11%)	0 (0%)	0.31 (NS)
Treatment			
PTCA	7 (17%)	0 (0%)	
CABG	35 (83%)	19 (100%)	0.09 (NS)

CABG = coronary artery bypass graft; CAD = coronary artery disease; CMR = cardiac magnetic resonance; ECG = electrocardiogram; EDVI = end-diastolic volume index; EF = ejection fraction; ESVI = end-systolic volume index; F = female; LBBB = left bundle branch block; M = male; MI = myocardial infarction; PTCA = percutaneous transluminal coronary angioplasty.

Strains and transmural extent of necrosis at baseline. Based on the 95% lower CI of Ecc obtained from normal volunteers (−10% mid-myocardial Ecc) (5) at baseline, 395 of all 672 segments were considered to have a normal function, whereas 277 segments were considered to be dysfunctional. We only considered the 256 dysfunctional segments subtended by significant (>50%) coronary stenosis. These dysfunctional segments were further separated into quartiles according to their mean transmural extent of necrosis (Fig. 2).

Coronary revascularization. Thirty-five patients underwent revascularization with CABG. The left anterior mammary artery was grafted to the left anterior descending coronary artery in all but 1 patient (n = 34) (who was a redo CABG). The right mammary artery (n = 11), free radial artery (n = 2), and gastroepiploic arteries (n = 3) were also used. Twenty-one patients received saphenous vein grafts. CABG revascularization was complete

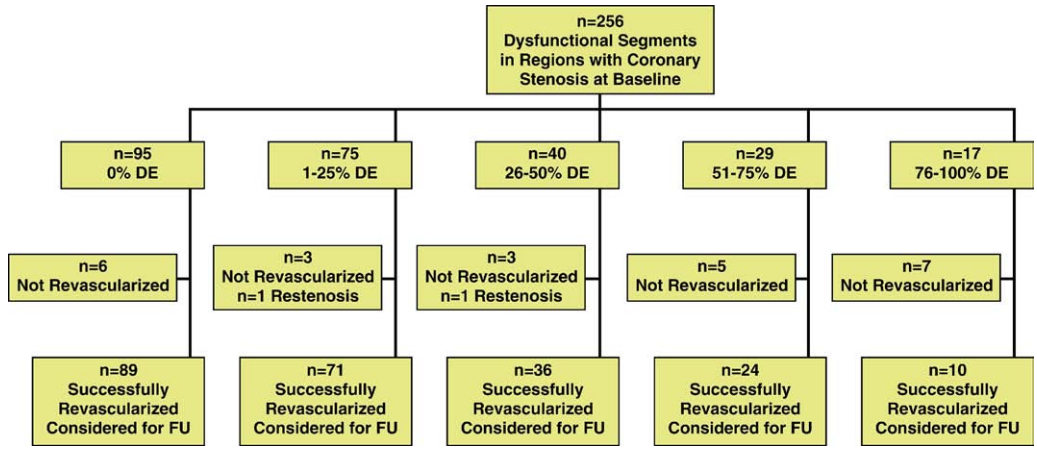

Figure 2. Distribution of Segments

The 256 dysfunctional segments having mid-myocardial circumferential shortening strain >−10% at baseline subtended by a significant coronary stenosis were stratified according to their mean transmural extent of necrosis (percentage of delayed enhancement [DE]). Segments with incomplete or failed were excluded. Only fully revascularized segments were considered for follow-up (FU).

(i.e., of all stenotic vessels) in all but 3 patients in whom the native vessels were too small to receive grafts. Seven patients underwent single (n = 6) or double angioplasty. Revascularization using angioplasty was complete in 3 patients and incomplete in 4 patients.

Completeness of revascularization was ascertained in 29 patients by MDCT and by 6 patients using repeat cardiac catheterization within 2 months of CMR. In the remaining 7 patients, renal insufficiency contraindicated MDCT for verification of vessel patency. Revascularization patency was verified in 6 of 7 patients undergoing angioplasty and in 28 of 35 patients undergoing CABG. No restenosis was found in the 6 patients who underwent angioplasty. Furthermore, all bypass grafts were found to be patent at the time of follow-up; however, in 1 patient with CABG, stenosis was found to be present angiographically in a native vessel situated beyond the graft. Overall, among the 256 dysfunctional segments at baseline, 24 segments were considered to not have been correctly revascularized and 2 revascularized segments were occluded (Fig. 2). These segments were excluded from analysis. Forty dysfunctional revascularized segments that lacked verification of their completeness were considered for analysis. At follow-up CMR, no patient presented with new infarcts, as demonstrated by regions of late DE not present at baseline study.

Improvement of strains after revascularization. Two typical patient studies are shown in Figure 3. Because 26 segments were considered to not have been correctly revascularized, only 230 dysfunctional segments were compared between baseline and follow-up. The distribution of mean transmurality of necrosis in these segments is shown in Figure 2.

Mean mid-myocardial, subendocardial, and subepicardial Ecc and mid-myocardial Err strain at baseline and follow-up in different types of segments are depicted in Figure 4 and Table 2. At baseline, mid-myocardial Ecc was not significantly different in dysfunctional segments with a different mean transmural extent of delayed hyperenhancement ($p = 0.07$ by analysis of variance). In the 395 nondysfunctional segments, Ecc or Err did not significantly change between baseline and follow-up. In the 230 correctly revascularized dysfunctional segments, mid-myocardial and epicardial Ecc and mid-myocardial Err improved after revascularization when necrosis at baseline was absent or when it occupied <25%, but not beyond ≥25% mean transmurality of necrosis. Subendocardial Ecc significantly improved in segments with up to 50% mean transmurality of necrosis. Significant, albeit poor correlations between mean transmurality of necrosis and recovery of mid-myocardial Ecc ($r = -0.33$, $p < 0.01$) but not with recovery of Err ($r = 0.09$, p = NS) in dysfunctional segments were observed. Results were similar when only segments belonging to patients with infarcts >1 year previously were considered.

ROC analysis (Fig. 5) demonstrated similar accuracy of the transmural extent of necrosis to predict improvement of mid-myocardial Ecc

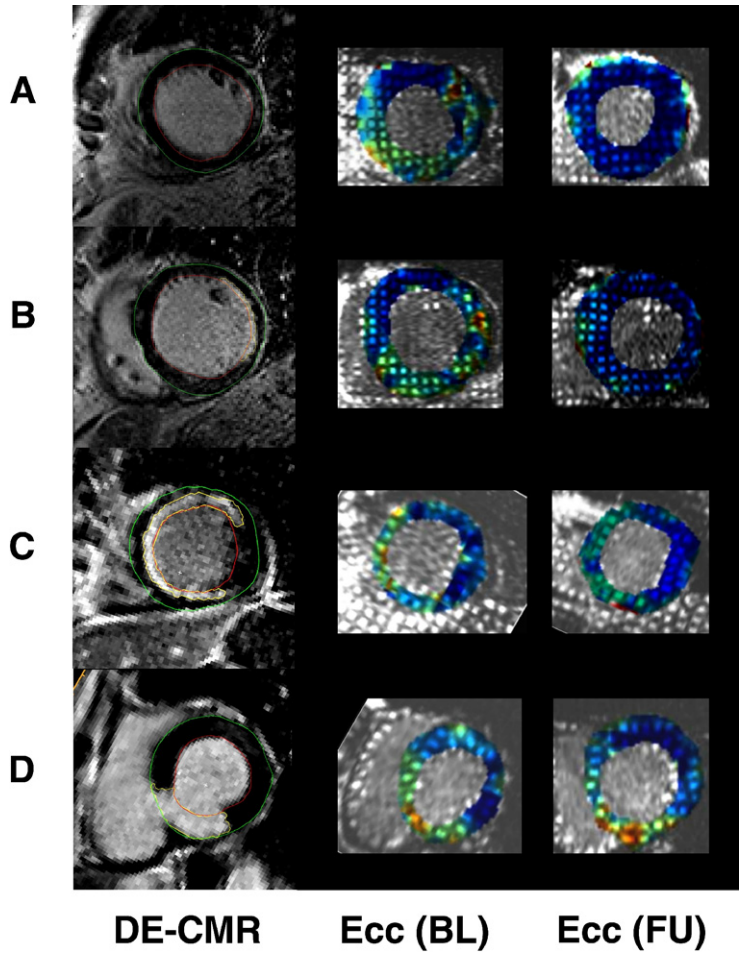

Figure 3. Examples of DE-CMR and End-Systolic Shortening Strain, Before and After Revascularization in 4 Representative Patients With Different Transmurality of Necrosis

Strain is color coded: green represents absence of contraction, blue normal shortening, and red abnormal elongation. **(A)** Absence of necrosis and inferior septal dysfunction, with recovery after revascularization. **(B)** Subendocardial scarring of lateral wall of <25% transmural extent. Inferior and lateral dysfunction at baseline recovered completely at follow-up. **(C)** Anterior, septal, and inferior subendocardial scarring with >50% transmurality of necrosis. Dysfunction persisted at follow-up. **(D)** Transmural inferior scarring with persisting dysfunction at follow-up. Ecc = Eulerian circumferential shortening strain; BL = baseline; other abbreviations as in Figures 1 and 2.

<−5% (area under the receiver-operator characteristic curve [AUC] = 0.67) normalization of Ecc to <−10% (AUC = 0.67), and normalization of Err to >7% (AUC = 0.64). Accuracy for predicting improvement of Err >8% was lower (AUC = 0.56, $p < 0.05$). Using an optimized cutoff value of ≥18%, mean transmurality had 54% sensitivity and 82% specificity for predicting recovery or nonrecovery of function to mid-myocardial ECC <−10% in dysfunctional segments at baseline.

The probability of improving Ecc by <−5% and that of normalizing to Ecc <−10% in dysfunctional segments at baseline after revascularization is shown in Figure 6. We observed that the probability of normalizing dysfunction steadily declined with each quartile of increasing mean transmurality from 62% for segments with 0% transmurality to only 10% for segments with >75% mean transmurality.

Improvement of global cardiac function after revascularization. LVEF improved significantly (from 35 ± 13% to 40 ± 7%, $p < 0.001$) after revascularization. This was due to a reduction of LV end-systolic volume (from 152 ± 78 ml to 133 ± 79 ml, $p < 0.002$), while LV end-diastolic volume remained unchanged (from 226 ± 79 to 213 ± 80 ml, $p = 0.12$). Patient symptoms improved from New York Heart Association functional class average 2.8 ± 0.7 to 1.6 ± 0.9 ($p < 0.001$).

EF before revascularization was significantly but inversely correlated with the number of dysfunc-

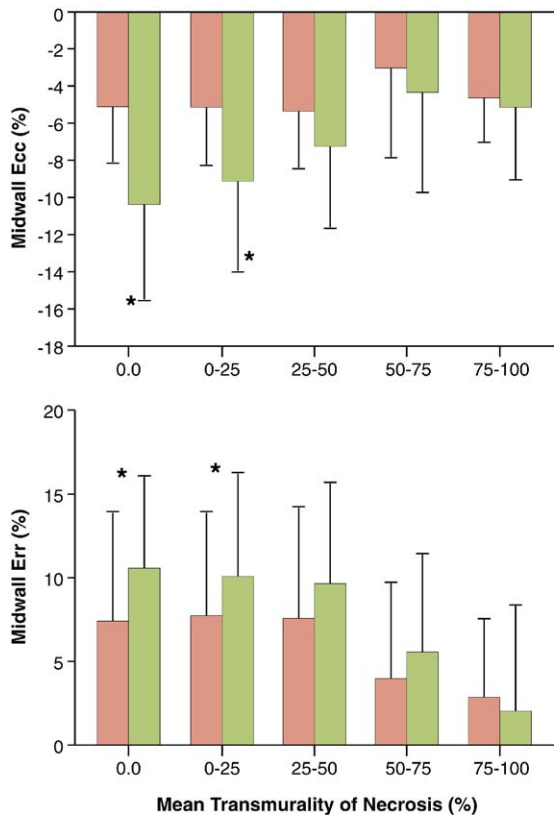

Figure 4. Strains Before and After Revascularization According to Transmurality of Necrosis

Mid-myocardial Ecc and Eulerian radial thickening strain (Err) in segments in normofunctional and fully revascularized dysfunctional segments of patients with variable amounts of myocardial necrosis before **(red bars)** and after **(green bars)** revascularization. *$p < 0.01$ after versus before revascularization. Abbreviation as in Figure 3.

tional segments at baseline ($r = -0.86$, $p < 0.001$). Similarly, EF after revascularization was significantly correlated with the number of segments remaining dysfunctional at follow-up ($r = -0.62$, $p < 0.001$). The change in EF between baseline and follow-up was correlated with the number of dysfunctional segments improving after revascularization ($r = 0.36$, $p < 0.02$). The change in EF after revascularization was, however, not significantly correlated with infarct size ($r = -0.11$, $p =$ NS) with the average transmurality in dysfunctional segments ($r = -0.11$, $p =$ NS) nor with the number of dysfunctional revascularized segments having <25% ($r = 0.26$, $p =$ NS), <50% ($r = 0.26$, $p =$ NS), and 75% ($r = 0.29$, $p =$ NS) mean transmurality of necrosis at baseline. ROC analysis demonstrated that presence of <4.5 dysfunctional segments with <75% mean transmural extent of necrosis had 67% sensitivity and 58% specificity to predict improvement of EF >5% after revascularization (AUC = 0.64). Diagnostic accuracy to improve EF >5% was similar in patients with lower EF (EF <35%, n = 22, AUC = 0.61, optimal sensitivity and specificity 73% and 61%, respectively) and in those with larger ventricles (end-diastolic volume indexed to body surface ≥100 ml/m^2, n = 20, AUC = 0.66 optimal sensitivity and specificity 71%/67%. Diagnostic accuracy to predict improvement of EF >5% was somewhat better in patients with infarcts older than 1 year (n = 29, AUC = 0.77, optimal sensitivity and specificity, 82% and 62%, respectively).

DISCUSSION

Our study demonstrated a quantitative yet complex relationship between improvement of regional strains in dysfunctional segments and transmural extent of necrosis. At mid-myocardial and epicardial level, Ecc and Err improved only up to 25% of the mean transmurality of necrosis. In contrast, in subendocardial levels, Ecc improved even when transmurality of necrosis was higher, up to 75%. Transmission of contractile forces and cross-fiber shortening from viable myocardium in noninfarcted subepicardial layers likely contribute to this effect in the subendocardium even when this layer is entirely infarcted.

The cutoff value of 25% for recovery of regional dysfunction at the mid-myocardial level was lower than that observed in earlier work (1,2,10,11) and also lower than what we previously observed in patients with acute myocardial infarction (12), in whom recovery of circumferential shortening occurred in segments with up to 75% transmurality of necrosis. This is likely explained by the fact that patients in our study were sicker, having lower EFs and higher LV volumes than those described by other groups in the literature. It is possible that in patients with more severely depressed cardiac function, more complex mechanisms such as tethering and remodeling are involved in dysfunction. Therefore, in such patients, recovery of dysfunction may only be achieved for lower transmurality of necrosis than in patients with less severe dysfunction and LV dilation. We already observed similar findings in previous work using positron emission tomography (13). Another explanation could be that our automated method computed the mean transmurality of necrosis, whereas others using visual assessment estimated the maximal transmurality of necrosis. When we computed maximal rather than mean

Table 2. Strains in Segments and Dysfunctional Segments With Variable Amount of Myocardial Necrosis at Baseline and After Revascularization

		Dysfunctional				
	Normofunctional (n = 395)	**0% Necrosis (n = 89)**	**1%–25% Necrosis (n = 71)**	**26%–50% Necrosis (n = 36)**	**51%–75% Necrosis (n = 24)**	**76%–100% Necrosis (n = 10)**
Ecc mid						
Baseline	−15.8 ± 3.7	−5.2 ± 3.0	−5.2 ± 3.1	−5.4 ± 3.1	−3.1 ± 4.8	−4.7 ± 2.3
Follow-up	−15.3 ± 4.7	−10.4 ± 5.2	−9.5 ± 5.0	−7.3 ± 4.4	−4.4 ± 5.4	−5.2 ± 3.9
p Value	0.06 (NS)	<0.001	<0.001	0.03 (NS)*	0.20 (NS)	0.64 (NS)
Ecc subendo						
Baseline	−16.2 ± 4.4	−6.5 ± 3.4	−6.3 ± 3.6	−6.0 ± 3.8	−3.1 ± 5.3	−3.8 ± 2.4
Follow-up	−15.7 ± 5.1	−10.8 ± 5.1	−10.4 ± 5.4	−8.1 ± 4.8	−6.5 ± 6.6	−5.0 ± 4.5
p Value	0.06 (NS)	<0.001	<0.001	0.004	0.01	0.45 (NS)
Ecc subepi						
Baseline	−13.9 ± 4.0	−5.1 ± 3.0	−4.9 ± 3.3	−4.6 ± 2.8	−3.3 ± 5.1	−3.8 ± 2.6
Follow-up	−13.3 ± 5.0	−9.2 ± 4.8	−8.1 ± 5.3	−6.2 ± 4.6	−4.7 ± 7.0	−4.1 ± 2.3
p Value	0.03 (NS)*	<0.001	<0.001	0.05 (NS)*	0.24 (NS)	0.80 (NS)
Err mid						
Baseline	+11.9 ± 6.4	+7.4 ± 6.6	+7.7 ± 6.2	+7.6 ± 6.6	+4.0 ± 5.8	+2.9 ± 4.7
Follow-up	+12.6 ± 6.4	+10.6 ± 5.6	+10.1 ± 6.2	+9.6 ± 6.1	+5.6 ± 5.9	+2.0 ± 6.4
p Value	0.03 (NS)*	<0.001	<0.01	0.12	0.47 (NS)	0.68 (NS)

*Considered nonsignificant given multiple comparisons.
Ecc = Eulerian circumferential shortening strain; Err = Eulerian radial thickening strain; Mid = mid-myocardial level; subendo = subendocardial level; subepi = subepicardial level.

transmurality of necrosis, mid-myocardial Ecc and Err increased up to 75% transmurality of necrosis.

The present study also confirmed earlier findings; that is, the high specificity (82%) of DE-CMR to predict the absence of functional recovery in transmural scars in relation to the presence of irreversible necrosis. Sensitivity for predicting recovery of regional dysfunction in segments with no or a small amount of necrosis was low (54%). In particular, not all segments and patients with viable myocardium had improved function after revascularization. There may be different explanations for this lack of

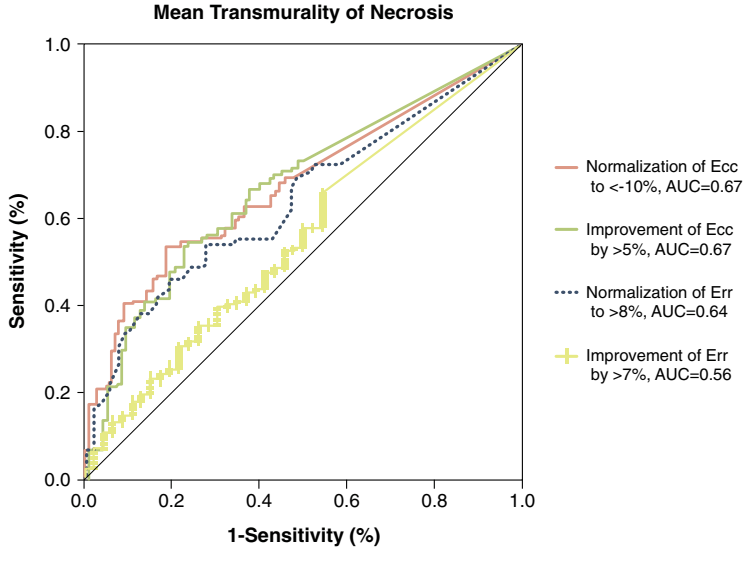

Figure 5. ROC Curves Evaluating Diagnostic Accuracy to Recover or Normalize Strains

Receiver-operator characteristic (ROC) curve evaluating diagnostic accuracy of mean segmental transmurality for predicting recovery of mid-myocardial Ecc (to <−10%), improvement of Ecc by <−5%, recovery of Err to >7% or improvement of Err by >8% in dysfunctional fully revascularized segments at baseline. AUC = area under the receiver-operator characteristic curve; other abbreviations as in Figures 3 and 4.

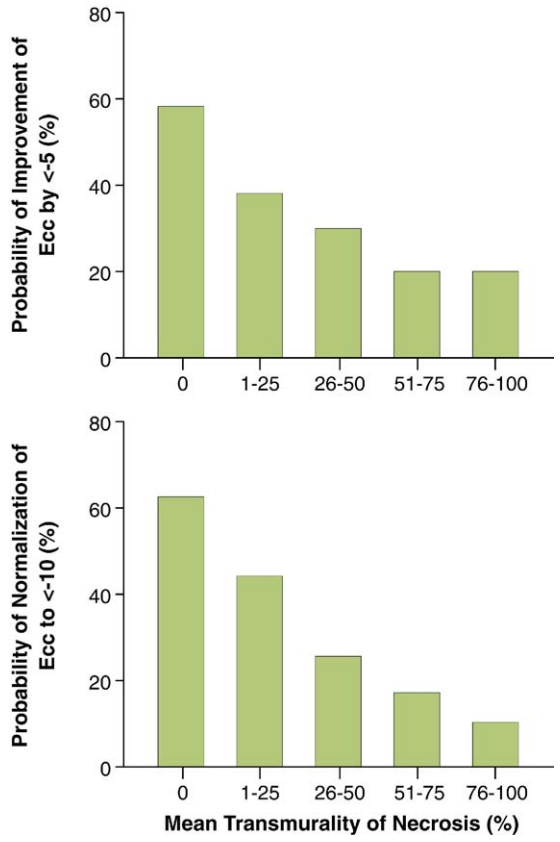

Figure 6. Probability of Normalizing or Recovering Dysfunction According to Transmurality

Probability of normalizing regional function to mid-myocardial Ecc <−10% **(A)** or of improving Ecc by <−5% **(B)** in dysfunctional fully revascularized segments with variable amounts of mean transmurality. Abbreviation as in Figure 3.

functional recovery of segments with no or a small amount of necrosis after revascularization. Successful revascularization is an important prerequisite to functional recovery of chronically ischemic myocardium. We ascertained the completeness of revascularization by MDCT or repeat cardiac catheterization in 83% of patients and excluded segments that were not completely revascularized or were reoccluded at follow-up. Therefore, this factor is unlikely to account for the low proportion of functional recovery in noninfarcted segments in our study. Periprocedural necrosis may also account for the absence of functional recovery at follow-up. However, we did not observe such periprocedural necrosis in the present study. Several studies (10,14,15) found that recovery of dysfunction in hibernating myocardium is not instantaneous, but rather a time-dependent phenomenon that may take as long as 1 year to complete. Because the average follow-up after revascularization in the present study was 10 months, insufficient follow-up is also unlikely to explain the low sensitivity of DE-CMR to predict functional recovery in noninfarcted segments. Therefore, we believe that other explanations might account for low functional recovery of some noninfarcted or small subendocardial scarring in our work and that of others. Mechanical factors such as passive tethering from neighboring transmurally necrotic segments or extreme LV remodeling may prevent functional recovery of noninfarcted segments, especially in severely dilated left ventricles with poor LV function, as in our study. Despite the presence of coronary artery disease, dysfunction in noninfarcted segments could also have resulted from other myocardial diseases (16), such as coexisting structural cardiomyopathy, which are not likely to improve after revascularization, or from as yet unidentified factors, accounting for the variable relationship between transmurality of necrosis and improvement of regional strain.

It is interesting to note that limited sensitivity to predict recovery of dysfunction has also been reported for nuclear imaging techniques (17). Therefore, some authors (3) suggested that demonstration of preserved inotropic reserve during stress dobutamine CMR might have better value for predicting functional recovery than demonstration of the absence of myocardial necrosis.

Clinical implications. The findings of the present study illustrate the complex relationship between regional viability and recovery of regional and global dysfunction. Although in our study, segments with ≥25% transmurality of necrosis had limited recovery of contractile function at the mid-myocardial and epicardial levels, EF and functional status improved even when necrosis was >25% transmural. Improvement of subendocardial shortening in those patients with more severe necrosis might have contributed to improvement of global function. Also, isometric tension development in subepicardial myocardium can contribute to tension development without any actual strain. This suggests also that revascularization of partially infarcted myocardium might have other beneficial effects beyond improvement of regional dysfunction. Some studies indicated that revascularization even in the absence of residual inotropic reserve may improve survival (18), presumably by restoring blood flow in subepicardial layers of nontransmural infarcts and reducing the potential to induce ventricular arrhythmias originating from the peri-infarct border zones (19,20). However, this has not been definitely proven. Thus, the presence of subendocardial scarring

on DE-CMR, which might indicate a low probability of recovery of regional contractile dysfunction, should probably not be a reason to withhold revascularization in patients with severe global dysfunction.

Study limitations. In this study, we only evaluated Ecc and Err but not longitudinal shortening and twist. Similar to other studies performing CMR at 2 different time points, misalignment of segments between the pre- and post-revascularization studies might have occurred. We attempted to minimize such misalignment error by careful registration of segments to fixed anatomic landmarks. Also, DE images (mid-diastole) and tagged images (throughout systole) were not acquired in the same part of the cardiac cycle. This could theoretically cause temporal misalignment due to through-plane motion. However, this likely had few repercussions because 1) our patients had a quite low EF and consequently low through-plane motion and 2) data from 2 to 3 adjacent slices were averaged to obtain strain and DE in 16 segments per patient. Although we took individual variations of coronary anatomy into account, the exact assignment of segments to coronary artery territories may be difficult, and some misregistration between segments and coronary territories might have occurred. Given that most patients had 3-vessel disease and were fully revascularized, we do not believe that this significantly influenced our study findings. Although we excluded segments from incompletely revascularized segments, we did not evaluate whether revascularized segments had improved perfusion after revascularization. That the lack of reperfusion at the tissue level may have contributed to reduced recovery of dysfunction in the present study cannot be excluded. Finally, the number of segments with >50% scarring was quite low, and our study might have been underpowered for detecting small increases in strain in these segments.

CONCLUSIONS

Our study evaluated the relationship between the quantitatively measured transmural extent of necrosis and improvement of regional function after revascularization. We demonstrated an inverse relationship between the transmural extent of DE and strain, yet with limited sensitivity for predicting recovery of regional dysfunction in segments without or with very little necrosis. Nevertheless, in this group of patients with severe LV dysfunction, we observed more beneficial effects of revascularization on improvement of global than on regional dysfunction. This illustrates the complex relationship that may exist between metabolic viability and functional recovery after revascularization.

Reprint requests and correspondence: Dr. Bernhard L. Gerber, Division of Cardiology, Cliniques St. Luc, Université Catholique de Louvain, Av. Hippocrate 10/2803, B-1200 Brussels, Belgium. *E-mail: bernhard.gerber@uclouvain.be.*

REFERENCES

1. Kim RJ, Wu E, Rafael A, et al. The use of contrast-enhanced magnetic resonance imaging to identify reversible myocardial dysfunction. N Engl J Med 2000;343:1445–53.
2. Selvanayagam JB, Kardos A, Francis JM, et al. Value of delayed-enhancement cardiovascular magnetic resonance imaging in predicting myocardial viability after surgical revascularization. Circulation 2004;1535–41.
3. Wellnhofer E, Olariu A, Klein C, et al. Magnetic resonance low-dose dobutamine test is superior to scar quantification for the prediction of functional recovery. Circulation 2004;109:2172–4.
4. Scanlon PJ, Faxon DP, Audet AM, et al. ACC/AHA guidelines for coronary angiography. A report of the American College of Cardiology/American Heart Association Task Force on practice guidelines (Committee on Coronary Angiography). Developed in collaboration with the Society for Cardiac Angiography and Interventions. J Am Coll Cardiol 1999;33:1756–824.
5. Gerber BL, Thanh HT, Roelants V, Pasquet A, Vancraeynest D, Vanoverschelde JL. Flow-function relationships in chronic left-ventricular ischemic dysfunction: impact of the transmurality of infarction. J Nucl Cardiol 2008;15:363–74.
6. Pouleur AC, le Polain de Waroux JB, Kefer J, Pasquet A, Vanoverschelde JL, Gerber BL. Direct comparison of whole-heart navigator-gated magnetic resonance coronary angiography and 40- and 64-slice multidetector row computed tomography to detect the coronary artery stenosis in patients scheduled for conventional coronary angiography. Circ Cardiovasc Imaging 2008;1:114–21.
7. Cerqueira MD, Weissman NJ, Dilsizian V, et al. Standardized myocardial segmentation and nomenclature for tomographic imaging of the heart: a statement for healthcare professionals from the Cardiac Imaging Committee of the Council on Clinical Cardiology of the American Heart Association. Circulation 2002;105:539–42.
8. Pereztol-Valdes O, Candell-Riera J, Santana-Boado C, et al. Correspondence between left ventricular 17 myocardial segments and coronary arteries. Eur Heart J 2005;26:2637–43.
9. Heiberg E, Sjögren J, Ugander M, Carlsson M, Engblom H, Arheden H. Design and validation of segment—freely available software for cardiovascular image analysis. BMC Med Imaging 2010;10:1.
10. Bondarenko O, Beek AM, Twisk JW, Visser CA, van Rossum AC. Time course of functional recovery after revascularization of hibernating myocardium: a contrast-enhanced cardiovascular magnetic resonance study. Eur Heart J 2008;29:2000–5.

11. Knuesel PR, Nanz D, Wyss C, et al. Characterization of dysfunctional myocardium by positron emission tomography and magnetic resonance: relation to functional outcome after revascularization. Circulation 2003; 108:1095–100.
12. Gerber BL, Garot J, Bluemke DA, Wu KC, Lima JA. Accuracy of contrast-enhanced magnetic resonance imaging in predicting improvement of regional myocardial function in patients after acute myocardial infarction. Circulation 2002;106: 1083–9.
13. Gerber BL, Ordoubadi FF, Wijns W, et al. Positron emission tomography using (18)F-fluoro-deoxyglucose and euglycaemic hyperinsulinaemic glucose clamp: optimal criteria for the prediction of recovery of post-ischaemic left ventricular dysfunction. Results from the European Community Concerted Action Multicenter study on use of (18)F-fluoro-deoxyglucose positron emission tomography for the detection of myocardial viability. Eur Heart J 2001;22:1691–701.
14. Vanoverschelde JJ, Depre C, Gerber BL, et al. Time course of functional recovery after coronary artery bypass graft surgery in patients with chronic left ventricular ischemic dysfunction. Am J Cardiol 2000;85: 1432–9.
15. Bax JJ, Visser FC, Poldermans D, et al. Time course of functional recovery of stunned and hibernating segments after surgical revascularization. Circulation 2001;104:I314–8.
16. le Polain de Waroux JB, Pouleur AC, Goffinet C, Pasquet A, Vanoverschelde JL, Gerber BL. Combined coronary and late-enhanced multidetector-computed tomography for delineation of the etiology of left ventricular dysfunction: comparison with coronary angiography and contrast-enhanced cardiac magnetic resonance imaging. Eur Heart J 2008;29:2544–51.
17. Vanoverschelde JL, D'Hondt AM, Marwick T et al. Head-to-head comparison of exercise-redistribution-reinjection thallium single-photon emission computed tomography and low dose dobutamine echocardiography for prediction of reversibility of chronic left ventricular ischemic dysfunction. J Am Coll Cardiol 1996;28: 432–42.
18. Pasquet A, Robert A, D'Hondt AM, Dion R, Melin JA, Vanoverschelde JL. Prognostic value of myocardial ischemia and viability in patients with chronic left ventricular ischemic dysfunction. Circulation 1999; 100:141–8.
19. Yan AT, Shayne AJ, Brown KA, et al. Characterization of the peri-infarct zone by contrast-enhanced cardiac magnetic resonance imaging is a powerful predictor of post-myocardial infarction mortality. Circulation 2006; 114:32–9.
20. Schmidt A, Azevedo CF, Cheng A, et al. Infarct tissue heterogeneity by magnetic resonance imaging identifies enhanced cardiac arrhythmia susceptibility in patients with left ventricular dysfunction. Circulation 2007;115: 2006–14.

Key Words: cardiac magnetic resonance ■ myocardial infarction ■ myocardial viability ■ strain.